ERDC/CRREL TR-16-10

US Army Corps of Engineers®
Engineer Research and Development Center

ERDC
INNOVATIVE SOLUTIONS for a safer, better world

Passive Gamma-Ray Emission for Soil-Disturbance Detection

Jay L. Clausen, Terrance Sobecki, Alexis L. Coplin, Terry D. Melendy, and Troy Arnold

August 2016

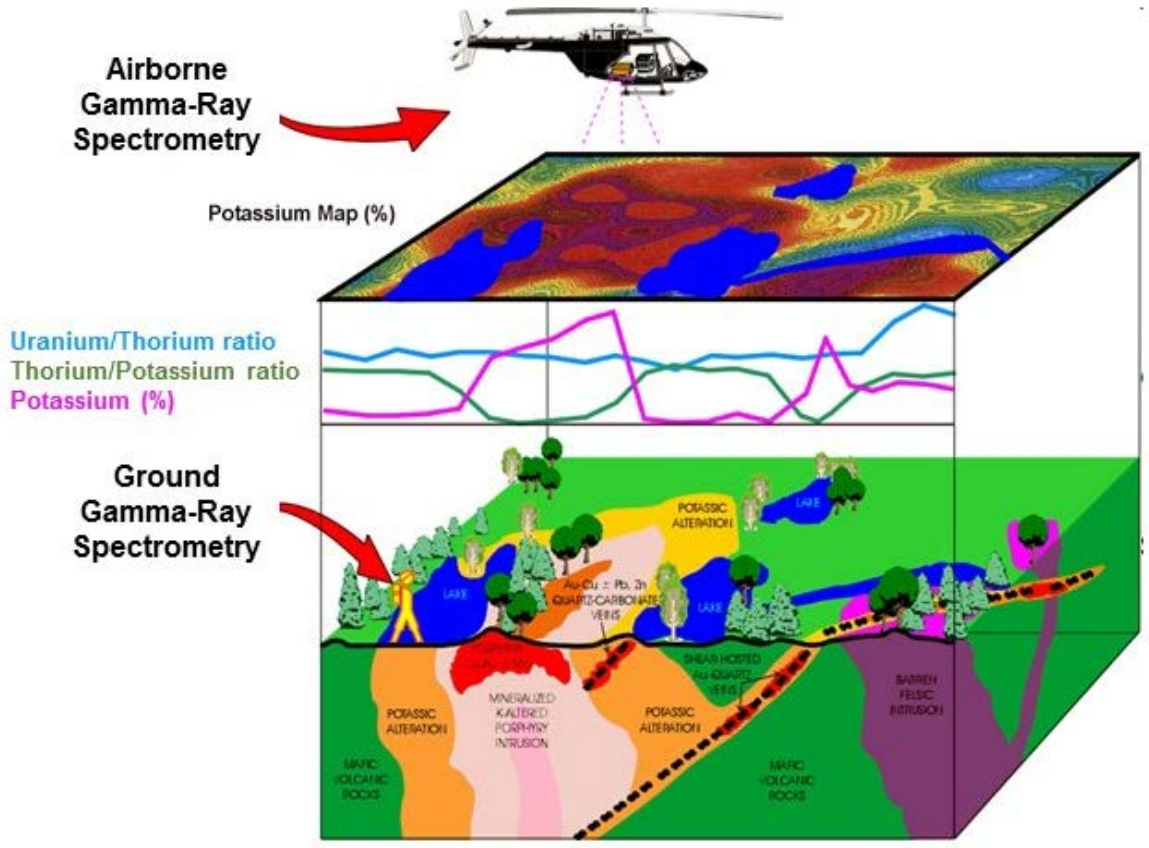

Cold Regions Research and Engineering Laboratory

The U.S. Army Engineer Research and Development Center (ERDC) solves the nation's toughest engineering and environmental challenges. ERDC develops innovative solutions in civil and military engineering, geospatial sciences, water resources, and environmental sciences for the Army, the Department of Defense, civilian agencies, and our nation's public good. Find out more at www.erdc.usace.army.mil.

To search for other technical reports published by ERDC, visit the ERDC online library at http://acwc.sdp.sirsi.net/client/default.

ERDC/CRREL TR-16-10
August 2016

Passive Gamma-Ray Emission for Soil-Disturbance Detection

Jay L. Clausen, Terrance Sobecki, Alexis L. Coplin, Terry D. Melendy, and Troy Arnold

U.S. Army Engineer Research and Development Center (ERDC)
Cold Regions Research and Engineering Laboratory (CRREL)
72 Lyme Road
Hanover, NH 03755-1290

Final Report

Prepared for Headquarters, U.S. Army Corps of Engineers
Washington, DC 20314-1000

Under PE0602784 Project 855, work unit "Large-Scale, High-Fidelity Remote Soil Property Variability"

Abstract

Human–terrain interactions, such as trafficking and excavation, cause changes to soil bulk density and porosity via compaction or mechanical bulking. The degree of compaction, as measured by bulk density, is a physical indicator of changing patterns of human–terrain interaction. Because soil radionuclide activity is a function of the mass content of the radionuclide and the volume of soil, the spectral signature of the naturally occurring soil radioisotope Potassium-40 (^{40}K) should be sensitive to changes in the soil bulk density and reflect the soil's disturbance history. If natural variations from geology and soil texture are systematic and predictable, one could map spatiotemporal bulk-density changes relative to some standard state as a metric of terrain disturbance. However, the natural variation in soil ^{40}K content is unknown and may confound density determinations via radionuclide activity measurements.

This study used a handheld sodium iodide gamma-ray detector to collect in situ gamma-ray spectra of four soils as a function of their potassium content, bulk density, texture, and water content. A statistically significant difference between the ^{40}K activity of uncompacted and compacted soil suggests that in situ ^{40}K gamma-ray emissions from soils are a sensor modality useful for soil-disturbance detection.

Contents

Figures and Tables

Figures

Tables

Preface

This study was conducted for the U.S. Army Corps of Engineers (USACE) Engineer Research and Development Center (ERDC) Basic Research Program under PE0602784 Project 855, work unit "Large-Scale, High-Fidelity Remote Soil Property Variability", Civilian-Military Operations/Human–Environment Interaction (CMO-HEI) work package. The technical monitor was Swathi Veeravalli.

This report was prepared by Dr. Jay Clausen, Alexis L. Coplin, and Dr. Terrance Sobecki (Biogeochemical Sciences Branch, Dr. Justin Berman, Chief); Terry D. Melendy (Force Projection and Sustainment Branch, Dr. Sarah Kopczynski, Chief); and Troy Arnold (Engineering Resources Branch, Jared Oren, Chief), U.S. Army Corps of Engineers (USACE) Engineer Research and Development Center (ERDC), Cold Regions Research and Engineering Laboratory (CRREL). At the time of publication, Dr. Loren Wehmeyer was Chief of the Research and Engineering Division. The Deputy Director of ERDC-CRREL was Dr. Lance Hansen, and the Director was Dr. Robert Davis.

COL Bryan S. Green was Commander of ERDC, and Dr. Jeffery P. Holland was the Director.

Acronyms and Abbreviations

^{22}Na	Sodium-22
^{40}K	Potassium-40
^{137}CS	Cesium-137
^{155}Eu	Europium-155
^{169}Yb	Ytterbium-169
^{241}Am	Americium-241
^{232}Th	Thorium-232
^{238}U	Uranium-238
As	Arsenic
Al_2O_3	Aluminum Oxide
ASCAT	Advanced Scatterometer
Ba	Barium
Bq	Becquerel (SI unit for activity, disintegration/second,)
Ca	Calcium
Ci	Curie (non-SI unit for activity, disintegration/minute)
Cr	Chromium
CMO-HEI	Civil Military Operations Human–Environment Interaction
Co	Cobalt
CRREL	U.S. Army Cold Regions Research and Engineering Laboratory
Cu	Copper
ERDC	Engineer Research and Development Center
Fe_2O_2	Iron Oxide

HESIM	Human–Environment Stability Indicator Model
HPGe	High-Purity Germanium
ICP-MS	Inductively Coupled Plasma–Mass Spectrometry
IED	Improvised Explosive Device
ISR	Intelligence, Surveillance, and Reconnaissance
K	Potassium
K_20	Potassium Oxide
keV	Kilo-Electron Volt
MeV	Million Electron Volts
Mg	Magnesium
Mn	Manganese
NaI	Sodium Iodide
Na	Sodium
Ni	Nickel
P	Phosphorus
pCi	Picocure (10^{-12} curies)
pCi/g	Pico Curries per Gram
SiO_2	Silicon Dioxide
Ti	Titanium
Tl	Thallium
USACE	U.S. Army Corps of Engineers
USEPA	U.S. Environmental Protection Agency
V	Vanadium
Zn	Zinc

Unit Conversion Factors

Multiply	By	To Obtain
cubic feet	0.02831685	cubic meters
picocurie	0.037	becquerel
degrees Fahrenheit	(F-32)/1.8	degrees Celsius
feet	0.3048	meters
foot-pounds force	1.355818	joules
inches	0.0254	meters
pounds (force)	4.448222	newtons
pounds (mass)	0.45359237	kilograms

1 Introduction

1.1 Background

Characterizing human–land interactions is critical to success in counterinsurgency and stability operations. Agricultural stability and capacity, hydraulic infrastructure, and natural-resource management all rely on measurements of soil physical properties. Additionally, the state of the ground and electro-optical and electromagnetic signatures require non-conventional soil properties (e.g., emissivity) as inputs for models. Such properties frequently depend on estimates of static physical soil properties, such as texture, grain size distribution, mineral content, etc. A knowledge gap exists in the local spatial variation of both conventional static properties and non-conventional properties. This problem is exacerbated in many military applications that require soil knowledge in denied areas, precluding direct measurement.

Human–terrain interactions, such as land management, trafficking, and excavation, can result in changes to soil bulk density and porosity via soil compaction or mechanical bulking. Thus, the degree of relative compaction of the soil (i.e., relative to the soil's natural uncompacted state or to the maximum obtainable density characteristic of the soil material as measured by the Procter [ASTM D698-12] or modified Proctor [ASTM D1557-12] density procedure [ASTM 2012a, 2012b; Diaz-Zorita et al. 2001]) can serve as a physically based indicator of changing patterns of human–terrain interaction. Consequently, compaction of soil from intrusive activities (e.g., vehicular and non-vehicular traffic) and disaggregation of soil as result of soil excavation (e.g., improvised explosive device [IED] emplacement) would be a useful phenomenon to exploit from a human–terrain interaction perspective.

Excavation and trafficking change the bulk density of natural soils and compacted lifts of soil used in roadbeds or building construction. If soil bulk density is a function of disturbance, then gamma-ray emission of the entire spectra or in a particular energy region of the spectrum characteristic of a specific radionuclide (Rossel et al. 2007) should differ between undisturbed and disturbed soil.

Remote, aerially extensive mapping of soil bulk density is conceivable via signatures of naturally occurring in situ soil radioisotopes such as potassium-40 (^{40}K) because the measured radionuclide activity in soil is a function of the mass of the radionuclide in the soil and the volume of soil material. However, the variation in the natural ^{40}K content of soils is unknown. The ^{40}K content is a function of soil parent material (surficial geological material) and soil texture (i.e., grain size distribution of the soil material); both of which may confound density determinations via radionuclide activity measurements. If the geological material and texture variations were systematic and predictable in terms of their influence on gamma-ray spectral signature of ^{40}K, it would be possible to map spatiotemporal changes in bulk density (i.e., relative compaction state) as a metric of terrain disturbance due to human influences.

Interest in passive detection of nuclear threats has driven the development of portable gamma-ray spectrometers (Kouzes et al. 2007), with high-purity germanium (HPGe) spectrometers commercially available (Feng et al. 2008; Vo and Russo 2002). Thallium-activated sodium iodide (NaI) detectors are most commonly used in airborne gamma-ray detectors (Paine and Minty 2005).

The soil mineralogy and soil-forming processes control the ^{40}K content of soil. Attenuation of ^{40}K gamma emissions is a result of scattering due to the water content and solid particle mass at any point in time or within the landscape. This scattering and attenuation is due to the photoelectric and Compton effects, both of which depend on material density, in addition to other factors (Hendriks et al. 2001). The combined mass attenuation effect of water and solid particles impacts the gamma-ray emissions within a material of given mineralogy (Rossel et al. 2007; Phogat et al. 1991; Jones and Carroll 1983). In practice, because the actual content of ^{40}K and other naturally occurring isotopes varies, the variation resulting from mass density differences (Blum 1997) may be hard to discriminate unless there is some knowledge of the surficial and underlying geology in the area and its relationship to ^{40}K content and distribution (Dickson and Scott 1997; Wilford et al. 1997).

Field soil nuclear density meters exploit the phenomenon of gamma-ray sensitivity to soil density and water content. Such meters make use of an active high-energy or external gamma-ray source, typically cesium-137

(^{137}Cs) either inserted into the soil from which direct gamma-ray transmission and attenuation is read or via backscatter from the soil surface after an active source has been directed onto it. To determine attenuation due to soil density, a need exists for a separate estimate of soil water content.

In the laboratory, spectra collected from two radioisotope sources, typically via a high-energy active source such as ^{137}Cs and a low energy active source such as ytterbium-169 (^{169}Yb) or americium-241 (^{241}Am), have been used to simultaneously determine soil water content and bulk density. The low-energy source is needed to factor out the impact of soil water content on the total attenuation of the high-energy source (Phogat et al. 1991). Again, this approach also relies on an active external source placed in close proximity to the soil surface.

The disadvantage of both techniques is the requirement of near direct contact of an external gamma-ray source with the soil. However, passive gamma-ray emissions from in situ radioisotopes are detectable via aerial surveys. These emissions are the result of radioisotopes found in the upper 35 cm of soil material (Paine and Minty 2005), though a majority of this, greater than 99%, comes from the upper 10 cm of the soil (Jones and Caroll 1983). If independent estimates of soil moisture content are available, as from satellite microwave-based systems such as the Advanced Scatterometer (ASCAT), then the bulk density of the soil and its relative state of compaction can theoretically be assessed for a given mineralogy and land cover. This assumes the soil moisture data is integrated with aerially sensed gamma-ray emissions of surficial material.

If an independent measure of soil water content is not available, then one must rely on a time series of gamma-ray measurements. Soil bulk density should be relatively constant under a given land cover or use (as a proxy for compactive effort). In addition, the mineralogy in a given area should be relatively constant if landform and provenance are known and controlled. As the soil dries out, the gamma-ray spectra should change over time as the contribution of water to the total mass attenuation changes. One should then be able to back out the soil density component of the total attenuation from such a time series.

Thus, by observing ^{40}K gamma emissions spatiotemporally across the terrain and conducting coherence and other spatial variance analyses, one

can create continuous geospatial datasets of soil density for given textural classes of soils without direct sampling. The typical gamma-ray aerial survey covers an area of approximately 600 m in diameter, depending on terrain and aircraft height. Work by others has shown submeter variability in soils for ^{40}K activity (Santo Júnior et al. 2005).

1.1.1 Nature of the problem

Detecting, characterizing, and predicting signs of human–terrain interactions have become critical components of intelligence, surveillance, and reconnaissance (ISR) activities in support of modern counterinsurgency and stability operations. Land use activities, such as agriculture and management of natural resources, transportation, and infrastructure development, aspects of the so-called patterns of life, are all influenced to some extent by the nature of the land surface and underlying soil. In turn, these patterns of life influence the land surface characteristics and leave their mark by altering the soil's physical and chemical properties (i.e., soil disturbance). Thus, the properties of the soil at or near the land surface present a potential suite of soil-disturbance indicators of human–terrain interaction. These markers may be manifested temporally, as before or after a particular human–land interaction event at a specific point in the terrain, or spatially as a result of the presence or absence of such activities taking place at numerous locations across wide swaths of terrain.

To use these indicators for ISR purposes, the knowledge gap between human activities at the surface of the soil and the nature of alteration of the underlying soil properties must be understood. This knowledge would allow selection of specific soil properties as indicators of ongoing or past soil disturbance and give those properties potential forensic value. To exploit this, development of an effective means of measuring the spatiotemporal changes in these properties is required. Ideally this would use stand-off methodologies deployable on existing equipment or personnel (i.e., handheld, ground vehicle, or aircraft) because many military applications require such intelligence in real time, in denied terrain, or over aerially extensive portions of the landscape.

1.1.1.1 Soil-disturbance indicators

Human-induced soil disturbance can alter both the chemical and physical properties of the soil (e.g., liming an agricultural soil changes the pH and

percentage base saturation while tillage of an agricultural soil alters the soil structure, consistence, and porosity). The military's interest involves anthropogenic physical disturbance of the soil surface caused by excavation, cut and fill, and trafficking. Therefore, soil properties that are susceptible to the processes of soil compaction (increasing the bulk density of the soil and decreasing the porosity) and the converse, mechanical soil bulking (decreasing the bulk density of the soil and increasing the porosity), are of interest. Changes in the spatiotemporal patterns of soil bulk density and porosity can be measured and attributed to either natural conditions, anthropogenically altered conditions reflective of normal patterns of life, or anomalies suggestive of a departure from natural conditions or normal patterns of life.

1.1.1.2 Soil structure and bulk density

Soil structure refers to the aggregation of primary soil particles (individual mineral grains or rock fragments) into secondary aggregates and the spatial arrangement of these aggregates to one another and to the pore space created. *Soil fabric* is a general term for the spatial arrangement of solid soil particles, soil aggregates, and the voids in a sample of soil (Brewer 1976). Soil structure is not directly measurable but can be descriptively conveyed categorically (Figure 1).

Figure 1. Classes of soil structure: (*A*) prismatic, (*B*) columnar, (*C*) angular blocky, (*D*) subangular blocky, (*E*) platy, and (*F*) granular (Soil Survey Staff 1951).

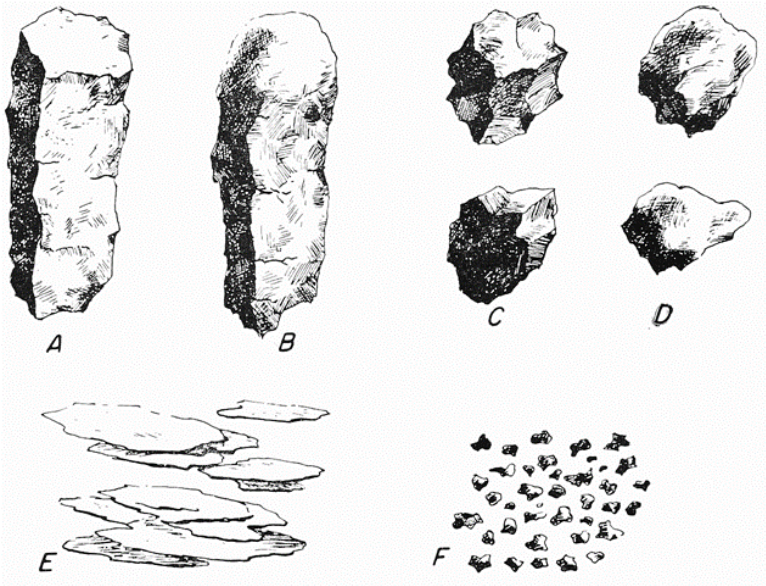

Soil bulk density, on the other hand, being defined as the weight of soil per unit volume of soil material, is a continuous, directly measureable property of the soil with units of weight/unit volume, typically g/cm^3 or kg/m^3 in the metric system and lb/ft^3 in English units. Soil porosity refers to the void space created by contact and packing of both primary soil particles and secondary soil aggregates in a unit volume of soil material. It is inversely related to soil bulk density as follows:

$$n = 1 - \frac{\rho_b}{\rho_s} \tag{1}$$

where

n = the decimal fraction of pore space in a unit volume of soil,
ρ_b = soil bulk density in units of g/cm^3 or kg/m^3, and
ρ_s = soil particle density (about 2.65) in units of g/cm^3 or kg/m^3.

Like soil structure, soil bulk density (and consequently soil porosity) changes in response to intentional or inadvertent manipulation of the soil resulting in compaction or mechanical bulking. Thus, soil bulk density is a use-dependent, temporarily variable soil property. A very rough guide is that a soil consists of approximately 50% solid soil particles and 50% pore space, which equates to a bulk density of approximately 1.32 kg/m^3. The soil pore space contains either air or water or both, depending on the soil water content. The volume of air-filled versus water-filled pore space changes as a function of precipitation or irrigation events and subsequent soil drying via deep percolation and evapotranspiration.

Undisturbed and agricultural soil bulk-density values typically fall within the range of 1.0 to 1.6 kg/m^3; but soils composed of volcanic ash and organic soils can have bulk-density values less than 1.0 g/cm^3, and soils heavily compacted or cemented by silica, iron oxides, carbonates, or salts can have values approaching 2.0 g/cm^3. Solid quartz sand particles and other silicate mineral grains have a density of approximately 2.65 g/cm^3. Because of soil structure and close packing limitations of individual primary soil particles and aggregates, a given volume of soil, even if highly compacted, always contains some proportion of pore space.

1.1.1.3 Soil compaction

Soil compaction refers to an increase in bulk density and a decrease in porosity relative to some *uncompacted* reference state or relative to adjacent surrounding soils in different states of relative compaction. Bulk density is sensitive to the compactive effort (the amount of force applied to the soil by a particular implement or action) associated with human–terrain interactions. These interactions typically stem from land management and trafficking. For example, agricultural cropping and tillage, grazing and pasturage, or forest land management and harvesting affect the density of the soil surface and even the subsoil layers because of implements used, the action of plant roots, and the numbers and types of grazing animals.

Excavation, cut and fill, and trafficking can not only change the bulk density of natural soils but can also change the bulk density of previously compacted soils, such as the compacted lifts of soil used in roadbeds or building foundation construction.

Excavation and cut and fill typically mechanically bulk the soil relative to its pre-disturbance state. Vehicular traffic will compact the soil relative to its pre-disturbance state in patterns specific to the vehicle type, weight, and frequency of travel. The same goes for foot traffic, though the degree of relative compaction may be less.

1.1.1.4 Soil bulking

A soil, whether in its natural state or previously compacted, can be *mechanically bulked*, meaning its bulk density is reduced via manipulation by natural or artificial means and that the percentage of pore space is increased. The best example of mechanical bulking is agricultural tillage, where the soil is mechanically disturbed with tillage implements to improve its workability and to increase porosity and available water holding capacity for crop production. In areas of military conflict, the digging, emplacement, and burial of mines or IEDs can also result in soil bulking when the devices are covered with fill. Any type of excavation and emplacement of fill changes the density of a soil at the surface and to the depth of excavation and fill emplacement compared to the surrounding unexcavated soil. Particularly, refilling an excavation typically results in bulking even if attempts are made to compact the fill material; and over

time, the bulk density of this *bulked* soil will increase due to settling and water consolidation from precipitation or irrigation events.

A natural mechanical bulking process in soils is freeze–thaw induced volume change. Also, some high-shrink–swell soils experience considerable volume change associated with wetting and drying. Bioturbation is another source of mechanical bulking resulting from burrowing of rodents, insects, or vegetation root penetration.

Thus, the change in soil bulk density in comparison with adjacent surrounding areas or over time is an indicator of soil disturbance by both natural processes and by intentional or inadvertent human activity such as trafficking, excavation, construction, food production, etc. Some activities lead to increases in bulk density, others to decreases.

1.1.1.5 Soil compactability

A soil's compactability refers to its ability to undergo a given increase in density as a function of compactive effort as opposed to its actual density at any one point in time or space. Compactability is not related to land cover or use but is an inherent soil property closely associated with the grain size distribution or texture of the soil (i.e., the relative percent of sand-, silt-, and clay-size particles making up the soil). Soil compactability is most commonly expressed with soil moisture–density curves, which plot the soil bulk density achieved by a given compactive effort as a function of water content. The maximum density obtained as a function of water content is termed the maximum dry density. This is the basis for the ASTM Proctor soil-density determination method (ASTM D698-12) and soil moisture–density curves (Diaz-Zorita et al. 2001). Indeed, soil compactability is quantified as the maximum dry density obtained in the Proctor density test (ASTM 2012b). A soil of a given texture at a given water content can be compacted only to its maximum dry density characteristic of a given compactive effort. Unlike bulk density, which is a use-dependent temporal soil property, soil texture and compactability are considered stable-static, use-invariant soil properties.

1.1.1.6 Soil compaction state

Soil compaction state is defined as the relative degree of compaction, as measured by bulk density, compared to some external standard, such as

maximum dry density, or to the degree of compaction of surrounding soils. It can serve as a physically based terrain-surface indicator of changing patterns of human–terrain interaction if allowances are made for the natural variation in soil bulk density relative to the soil's maximum dry density. Some of this variability is systematic. For example, landform and surficial material provenance are good predictors of soil texture and mineralogy and thus provide some predictive constraints on the soil density values achievable in a given area and hence on the maximum dry-density property of the soil. The texture of surficial soil materials in a region can be predicted and mapped from knowledge of the surficial geology and geomorphology and interpretation of satellite or airborne imagery patterns, textures, and tone. Thus, soil compactability is mappable as a stable static feature of the soil cover of a region's terrain.

By mapping the spatiotemporal distribution of the use-dependent temporal property of soil bulk density and comparing that to the spatial map of the stable static use invariant property of soil compactability (e.g., Proctor maximum dry density) one could estimate the soil's relative compaction and potentially use it as a direct indicator of changing patterns of human–soil interactions. The challenge is finding a means of measuring or mapping soil bulk density remotely for the above scenario to be feasible. Such soil processes and properties could then be parameterized as part of the Civil Military Operations Human–Environment Interaction (CMO-HEI) work package for use in the Army's Human–Environment Stability Indicator Model (HESIM).

1.1.2 Gamma-ray emission spectrometry and soil bulk-density measurement

It is not the purpose of this section to give an exhaustive background on radioisotope chemistry and physics. Rather, sufficient background information is presented on the application of gamma-ray spectrometry to soil density measurement so the reader understands the conceptual underpinnings and can better assess the results presented in the report.

Both soil structure and bulk density are key soil properties that influence the state of the ground as it impacts electro-optical and electromagnetic sensor signatures. For example, differential scattering of short-wavelength radar waves by surface soil roughness (i.e., structure) and the alteration of

soil thermal emissivity (as measured by thermal infrared sensors) from soil compaction or bulking change the soil pore-space ratio and the soil water state (the amount of water held in the soil relative to saturation).

Scanning radar and thermal imaging are two techniques used to infer soil disturbance. However, these methods are subject to many interferences: the angle of incidence of the radar beam caused by changes in topography or elevation, scattering due to vegetation structure, attenuation due to precipitation events, shading and water dynamics causing spatiotemporal change in soil temperature, and heat flux outside of normal diurnal patterns. It would be advantageous to be able to measure soil bulk density directly as an indicator of soil disturbance rather than via inference from some secondary or tertiary derivative property of the land surface.

Soil bulk density can easily be measured by taking a sample of the soil back to the laboratory and weighing it and determining its volume by water displacement. Measurements of soil bulk density can also be obtained in situ by water or sand displacement of a small excavation or by correlation with soil penetration resistance or soil shear-strength measurements. However, these techniques require access to the area of interest to collect a sample or to make a measurement. A standoff method conceptually akin to radar or thermal infrared techniques would be more suitable.

The absolute value of the soil bulk density that is achieved by the compaction or bulking process is not the focus. Rather, interest lies with the detection of the relative change of soil bulk density as an indicator of excavation or trafficking relative to some internal or external reference state. Ultimately, the objective is to assess the soil compaction state.

If the soil bulk-density variation across a given area of interest is evaluated as a spatial random field (Christakos 1992), the goal is to identify relative spatiotemporal changes in soil bulk density and its variability indicative of patterns of life and more importantly anomalies suggestive of activities outside of the normal day-to-day patterns. To identify these relative spatiotemporal changes, one reference state is the bulk density of the soil under natural vegetation. An undisturbed area of interest can be used as a reference to infer the magnitude and direction of man-induced bulk-density changes. Thus, a set of soil bulk-density values from a landscape can be analyzed as a vector spatial random field (Vanmarcke 1983) to determine

the direction of change (increase or decrease in magnitude in a certain direction across the landscape), with the reference state being contained within the dataset itself as an internal standard.

Another reference state is the maximum dry-density characteristic of the soil material as measured by the Proctor (ASTM D698-12) or modified Proctor (ASTM D1557-12) density procedure (ASTM 2012a, 2012b; Diaz-Zorita et al. 2001). This is an example of an external reference as soils differ in their maximum attainable dry density as discussed previously. Through laboratory measurements, soil bulking can be inferred relative to the maximum obtainable dry density for each soil type in a given area. However, anomaly detection due to bulking of a natural or previously compacted soil would not be discernable in the field. Another disadvantage of this approach is the requirement of additional knowledge about the area of interest in the form of soil types and maximum dry density. An analysis of variance of the bulk density in the area of interest, using an undisturbed area as an internal reference, requires no such a priori knowledge.

So where do soil radionuclides and gamma-ray emissions from the soil come into play? Gamma rays are the most energetic form of electromagnetic radiation next to cosmic rays (Figure 2).

Figure 2. The position of gamma rays relative to the rest of the electromagnetic spectrum.

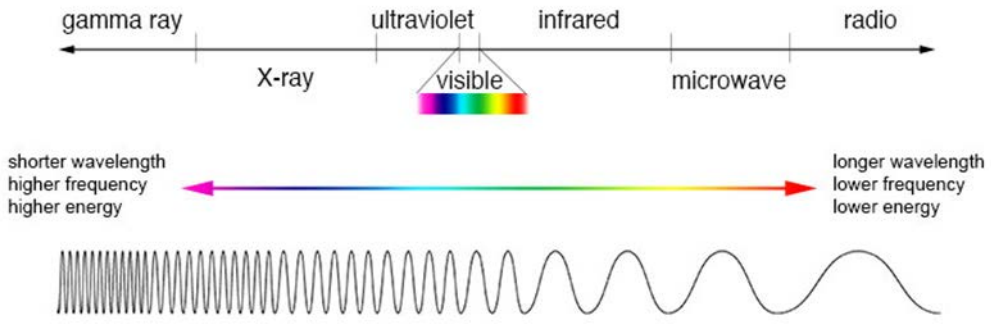

Gamma rays are emitted by various radionuclides (i.e., radioisotopes) that occur naturally in the soil. While gamma rays produced by radioactive decay of radioisotopes are energetic enough to pass through many solid materials, they can be differentially attenuated or their pathway altered by soil constituents (soil solids, air, and water) and other absorbers, a process

often called *recoil*. Attenuation is a function of the cross-sectional composition and thickness of potential absorbers that the gamma rays must pass through. This same process, however, provides a means of measuring relative volume differences in soils (i.e., changes in soil bulk density) by using gamma-ray attenuation because changes in soil bulk density change the ratio of solids:air:water in a given volume or cross-sectional area of soil.

This report looks at the in situ gamma-ray emission spectra from the terrain soil surface as an indicator of bulk-density change, specifically emissions from the ^{40}K. Other naturally occurring radioisotopes that contribute to soil-surface gamma-ray emissions include uranium-238 (^{238}U) and thorium-232 (^{232}Th) although these elements are in much lower abundance and have complex decay pathways (Minty 1997). Potassium has a higher crustal abundance, is ubiquitous in geological materials, has a relatively simple decay path (Paine and Minty 2005; Wilford et al. 1997), and is much more amenable to inference of soil bulk density for our purposes.

The phenomenon of gamma-ray sensitivity to soil density and water content is exploited in use of field-deployed nuclear-density meters. Such meters make use of an active high-energy external gamma-ray source, typically ^{137}Cs, either inserted into the soil and from which direct gamma-ray transmission and attenuation is read or via backscatter from the soil surface after an active external source has been directed onto it. Determining attenuation due to soil density needs a separate estimate of soil water content as water can also absorb gamma rays.

In the laboratory, spectra collected from dual sources have been used to simultaneously determine soil water content and bulk density, typically via a high-energy external source such as ^{137}Cs and a low energy active source such as ^{169}Yb or ^{241}Am. The low-energy source is used to factor out the impact of soil water content on the total attenuation of the high-energy source (Phogat et al. 1991). Again, this approach also relies on an active external source placed in close proximity to the soil.

The disadvantage of both techniques is that they require direct contact of an external gamma-ray source with the soil. However, passive gamma-ray emissions from in situ radioisotopes are detectable via aerial surveys or handheld gamma-ray spectrometers. These emissions are the result of radioisotopes found predominantly in the upper 35 cm of soil material

(Paine and Minty 2005), though a majority of these emissions, greater than 99%, come from the upper 10 cm of the soil (Jones and Caroll 1983). An ideal in situ gamma-ray source is potassium. Potassium makes up approximately 2.6% of the earth's crust, with ^{40}K approximately 0.01% of the total potassium; and it is ubiquitous in its distribution. In rocks and soil material, most of this potassium is found in feldspars, mica, and clay minerals. Thus, the natural background counts of ^{40}K will vary depending on the underlying geology and its mineralogical composition.

1.1.3 Radiochemistry of Potassium

^{40}K decays to stable argon (^{40}Ar) gas, emitting a beta particle (β) and a gamma-ray photon (γ) of 1.46 million electron volts (MeV) energy (Equation 2):

$$^{40}K \rightarrow Ar(stable) + \beta + \lambda(1.46MeV) \quad (2)$$

The ^{40}K activity of pure elemental potassium, which contains approximately 0.01% ^{40}K, is 816 to 838 pCi/g. A rate of 1 disintegration/second is defined as the becquerel (Bq), the SI unit for activity. The traditional (i.e., non-SI) unit of activity is the curie (Ci), which is 3.70×10^{10} disintegration/minute and is the amount of activity produced by the decay of 1 gram of ^{226}Ra. Equation (3) provides the relationship between becquerels and curies:

$$1 \text{ Bq} = 27.0270 \text{ pCi} \quad (3)$$

The picocurie (pCi), 10^{-12} curies, is a more useful non-SI unit because of the lower rates of decay measured in the field due to the relatively low crustal abundance of naturally occurring radioisotopes. The pCi unit is used throughout the text as it gives reasonable numerical magnitudes for the activity levels measured.

A typical soil has a ^{40}K activity of approximately 20 pCi/g, reflecting the fact that the soil is not pure potassium but a mixture of different elements. The activity of ^{40}K is influenced by not only the potassium content of the soil but also the soil bulk density. This is because the major soil constituents of air, water, and solid soil particles all have different gamma-ray mass attenuation coefficients. As mentioned in the previous section,

changes in soil bulk density affect the makeup of a given cross-sectional area through which in situ emitted gamma rays must pass on their way to the soil surface (Figure 3).

Figure 3. Schematic of ^{40}K attenuation pathways in compacted versus uncompacted or mechanically bulked soil.

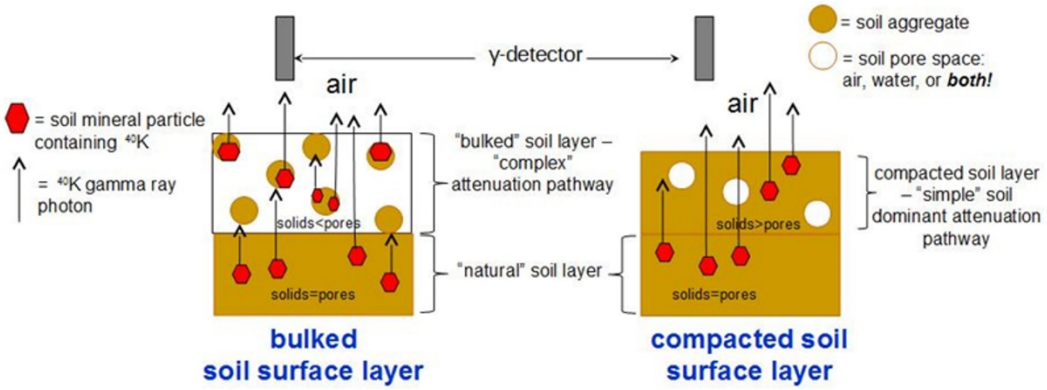

The term *activity* refers to the disintegration rate of the respective radioisotope, ^{40}K in the above Equation (2). Radioactive decay is a first-order reaction with activity (A) being equal to the number of radioactive nuclei present at any given time (N), which is a radioisotope-specific disintegration constant (λ) in Equation (4). Because λ is a rate constant, it has the units of $-t$:

$$A = \lambda N \tag{4}$$

Thus, activity represents the number of disintegrations per unit time and is a function of the initial activity at any given time, t_0, and an exponential decay function at some later time, t (Equation 5):

$$A = A_0 e^{-\lambda t} \tag{5}$$

where

A = activity,
A_0 = activity at time t_0,
E = natural log to the base e,
λ = disintegration rate constant, and
t = time.

The various radionuclides emit gamma rays of different energies upon decay, thus the gamma-ray spectrum can be represented by the activity (typically measured in counts) of a particular radioisotope versus the energy of the gamma-ray photons emitted (Figure 4).

Figure 4. Generalized gamma-ray spectrum showing peaks at various energy levels that are characteristic of different radioisotopes.

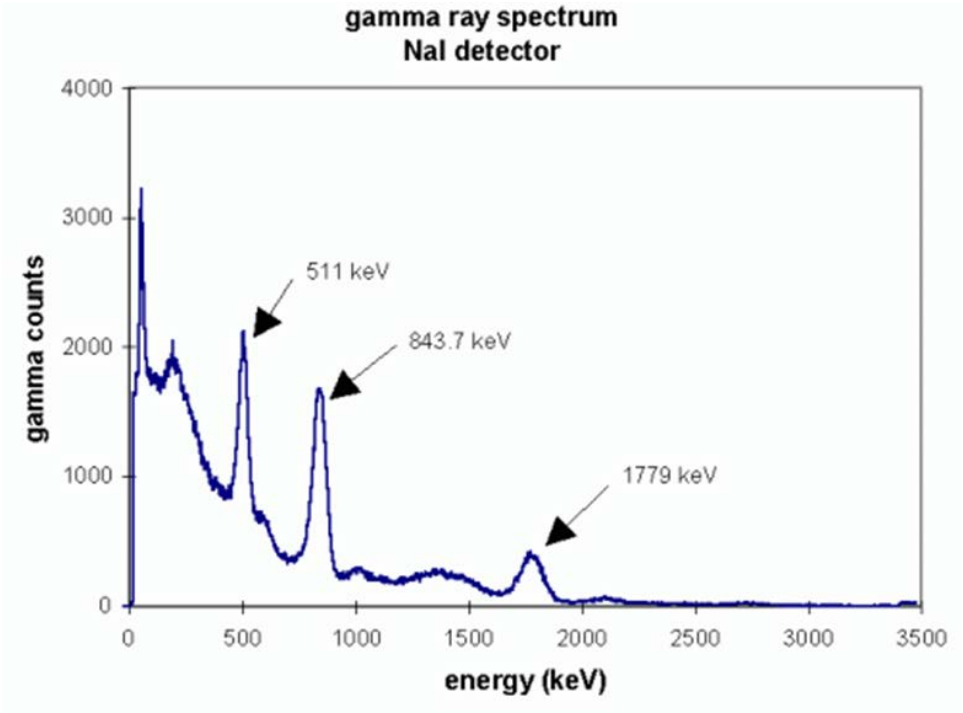

Thus, the spectra are the finger prints of particular radioisotopes in the soil or other sample material.

1.1.4 Application of gamma-ray spectrometry to the problem

The above radiochemistry enables the analysis and identification of radionuclides in soils and other earth materials by means of gamma-ray spectrometers (Feng et al. 2008; Santo Júnior et al. 2005; Kinno et al. 2002), including via aerial survey (Lyons and Hendricks 2006; Wilford et al. 1997; Hopkins 1996). Interest in passive detection of nuclear threats has driven the development of portable gamma-ray spectrometers (Kouzes et al. 2007), with HPGe detector spectrometers commercially available (Feng et al. 2008; Vo and Russo 2002). Thallium-activated NaI detectors are most commonly used in airborne gamma-ray detectors (Paine and Minty 2005).

The activity of a radionuclide in soil layer i (A_i) is a function of the volume and mass of soil in a given layer (Feng et al. 2008) as shown by the volume integral in Equation (6):

$$A_i = \iiint A_{i,v} dV \iiint A_{i,m} \rho dV \tag{6}$$

where

$A_{i,v}$ = unit volume radionuclide activity in soil layer i,
$A_{i,m}$ = unit mass radionuclide activity in soil layer i, and
ρ = soil bulk density.

As mentioned in Section 1.1, the geometry (i.e., the fabric) of the potassium distribution in the soil determines the total counts received by the spectrometer because the measured activity of ^{40}K is attenuation-pathway controlled (Figure 3). The attenuation is a function of the mass attenuation coefficients of the soil constituents (i.e., soil, water, and air) found in a unit cross-sectional area of the soil surface. Soil bulk density and water content determine the proportions of the different constituents in a given cross-sectional area.

Soil bulk density and porosity are very sensitive to human use and disturbance of the soil. They are also key land-surface parameters that impact ecological, hydrological, and earth–atmosphere energy transfer processes. Knowing the spatial-temporal distribution of ^{40}K gamma-ray emissions from the soil surface in relationship to patterns of human land-use activities provides a physically based terrain-surface indicator of human–terrain interaction, provided one can account for the effects of potassium content and soil water content variation.

1.1.5 Relationship of gamma-ray emission from soils and soil compaction state

Because soil bulk density is affected by soil disturbance, changes in the magnitude of ^{40}K gamma-ray emissions from the soil surface in theory allow differentiation between an undisturbed and disturbed soil (Rossel et al. 2007).

Potassium is a ubiquitous soil constituent found in clay minerals of the fine fraction and feldspars and micas of the coarser sand and silt fractions. Soil mineralogy and soil forming processes control the potassium content and thus the ^{40}K content of the soil, but the attenuation of ^{40}K gamma-ray emissions by the soil is a function of the actual mass of soil water and solid particles at any point in time in the landscape and their influence on scattering and attenuation of the gamma rays, as shown previously in Figure 3. For ^{40}K, this scattering and attenuation is due to the photoelectric and Compton effects, both of which depend on material density in addition to other factors (Hendriks et al. 2001). The combined mass attenuation effect of water and solid particles is reflected as gamma-ray emission sensitivity to soil water content and soil bulk density within a material of given mineralogy (Rossel et al. 2007; Phogat et al. 1991; Jones and Carroll 1983).

In practice, because the actual content of ^{40}K and other naturally occurring isotopes varies, the variation resulting from mass density differences (Blum 1997) may be hard to discriminate unless there is some knowledge of the surficial and underlying geology in the area and its relationship to ^{40}K content and distribution (Dickson and Scott 1997; Wilford et al. 1997). Remote, aerially extensive mapping of soil bulk density is conceivable because the measured activity of ^{40}K in soil is a function of the mass of the radionuclide in the soil and the volume of soil material, as discussed previously (see Equation 6). However, it is also a function of the inherent potassium content of the soil material, with different geological materials having different mineralogical provenance.

The variation in the natural ^{40}K content of soils is often an unknown for a given area of influence. If the geological material is systematic and predictable, in terms of their influence on gamma-ray spectral signature of ^{40}K, it is possible to map spatiotemporal changes in bulk density (i.e., relative compaction state) due to human influences. In soil-disturbance detection, however, interest is mostly on the microscale (Christakos 1992) variability in ^{40}K between disturbed and adjacent undisturbed soil. Thus, the variability of the soil potassium content at the macroscale (i.e., due to regional surficial geology) in a random field of ^{40}K measurements (Christakos 1992) may not be a significant confounding factor for such an application.

If an independent measure of soil water content is not available, then one might rely on a time series of gamma-ray measurements. Soil bulk density

should be relatively constant under a given land cover or use (as a proxy for compactive effort) over short periods of time while soil water content will vary. If the soil dries out, the gamma-ray spectra should change over time as the contribution to the total mass attenuation by the water changes. One should then be able to back out the soil density component of the total attenuation from such time series.

Thus, by observing ^{40}K gamma emissions spatiotemporally across the terrain and conducting coherence and other spatial covariance analyses considering the dataset as representing a random field (Christakos 1992; Vanmarcke 1983), one can theoretically create continuous geospatial datasets of soil density for given textural classes of soils without direct sampling and that represent regional macroscale patterns of soil bulk density due to surficial geology and broad land-cover use patterns. However, we are typically interested in smaller areas or subareas of a particular area of influence. In addition, the typical commercial gamma-ray aerial survey covers an area of approximately 600 m in diameter, depending on terrain and aircraft height; but work by others has shown submeter variability in soils for ^{40}K activity (Santo Júnior et al. 2005). Thus, finer-scale or ground-based measurements over smaller areas could result in detection of anomalies associated with recent anthropogenic soil disturbance.

1.2 Objective

The objective of this study was to determine if passive gamma-ray emissions from the ^{40}K radioisotope in soils are sensitive enough indicators of soil bulk-density change to identify the relative state of soil compaction as a sign of soil disturbance. Relative compaction state for a small area of uniform soil type can be defined as the microscale variability in soil density as a function of the pattern of natural and undisturbed areas of the soil surface versus adjacent physically disturbed areas, such as compacted roadbed tire tracks, areas of cut and fill, etc. Comparing and contrasting this microscale variability to the overall macroscale variability of a vector spatial random field (Christakos 1992) of soil bulk density or gamma-ray measurements should pinpoint a localized soil disturbance associated with excavation or burial.

Our specific objective is to consistently detect soil bulk-density or compaction-state differences by using a handheld gamma-ray spectrometer and a

series of known-density soil samples of different composition and properties (Figure 5). This is a prerequisite to using gamma-ray spectrometry as a sensor mode for stand-off soil-disturbance detection as per Figure 5. The ability to detect statistically significant differences in soil bulk density in the laboratory via in situ ^{40}K soil gamma-ray emissions would suggest it is feasible to conduct plot or field studies of the standoff methodology.

Figure 5. Conceptual approach for identifying areas of impacted soils.

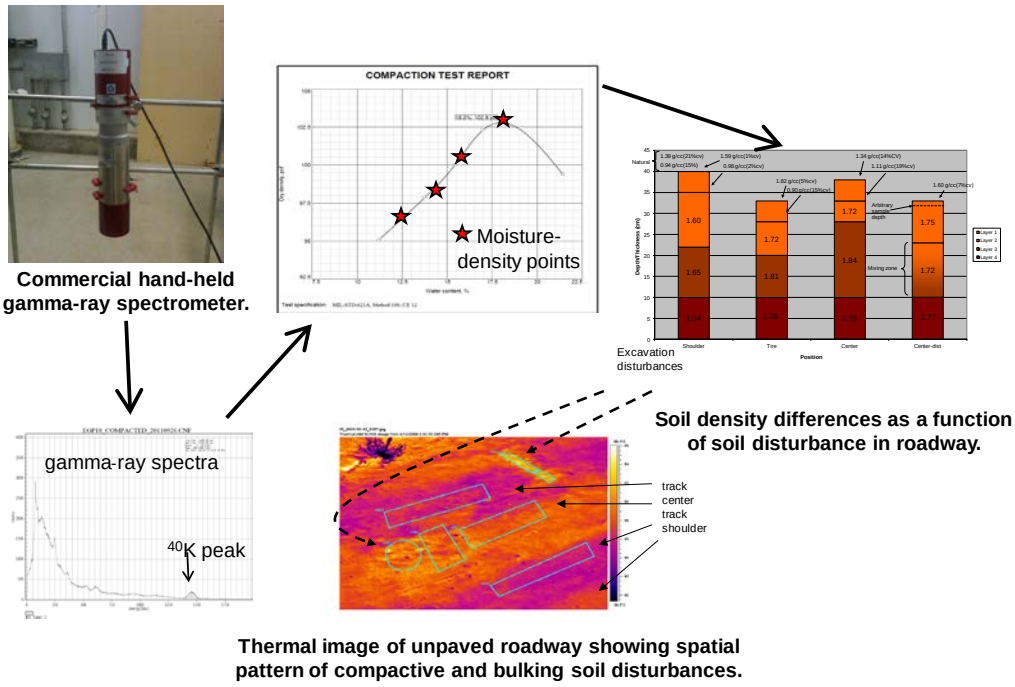

1.3 Approach

The approach used for this project was to characterize the ^{40}K gamma-ray emissions of four soils as a function of soil density and moisture content. Soil density was varied by compacting or bulking the soil. The moisture content was controlled by adding water to the soil.

Figure 5 contains the fundamental components of the study. The study used a handheld gamma-ray spectrometer to collect gamma-ray spectra in the laboratory from soil samples that represent field soils prepared to different relative states of compaction. Experimental treatments included soils compacted to various compaction levels up to and including the maximum dry density, achieved from application of the ASTM methods de-

scribed previously. Additional treatments consisted of mechanically bulking and changes to soil moisture content. The sensitivity of the ^{40}K emission peak, in terms of activity, was ascertained relative to various potential interferences, such as soil texture, potassium content, and soil water content. If statistically significant relationships between the resulting soil bulk density and ^{40}K activity can be identified across the range of soil texture, potassium content, and soil water content, the hypothesis will be accepted. Acceptance of the hypothesis means that changes in soil ^{40}K activity are a potential measure of physical soil disturbance associated with mechanical compaction and bulking. It also suggests field investigations attempting to map such changes with handheld standoff instrumentation to identify disturbance patterns are warranted. This result would specifically support the "Large-Scale, High-Fidelity Remote Soil Property Variability" work unit under the CMO-HEI work package, including the following examples:

1. Determining methods to characterize wide-area soil-property variability without requiring direct sampling
2. Generating more accurate battlefield analysis from tactical decision aids driven by soil properties
3. Creating a continuous surface of soil properties
4. Relating multisource remote geophysical signatures to landscape processes and soil properties.

2 Methods

2.1 Materials

Four soils of varying texture and elemental composition were selected for use in the study and varied from a silty clay to sand (Table 1). Potassium content, reported as percent potassium oxide (K_2O), varied for each of the soils also. Soil names are merely contrived names based on the sampling location or storage area from which the soil material was obtained. All the soil materials used, however, are from samples of soil taken in the field. The goal was to obtain a set of soils representing a range in textures and potassium content, as opposed to trying to represent real-world soils as part of specific terrains.

Soil particle size distribution (i.e., soil texture) was determined via the hydrometer method, ASTM D422-63 (ASTM 2007). The metal content of the soils was determined by acid digestion and inductively coupled plasma–mass spectrometry (ICP-MS) using USEPA method 3050B (USEPA 2016). Appendix A contains additional analytical data on the soils.

Table 1. Selected physical and chemical properties of the soil material used in this study[1] reported as percents.

Soil Name	Sand	Silt	Clay	Soil Type[2]	Fe_2O_3	Al_2O_3	SiO_2
Cemetery	94.5	5.5	0	Sand	2.1	14.4	54.2
EGP	20.3	63.2	16.5	Silt loam	6.5	14.2	61.3
South Bin	7.2	46.9	35.9	Silty Clay	5.8	14.7	65.8
North Bin	59.2	31.1	9.7	Sandy Loam	5.1	12.5	75.5

Fe_2O_3 = iron oxide; Al_2O_3 = aluminum oxide; SiO_2 = silicon dioxide

[1] Soil particle size analysis reported on a percentage of the fine-earth (i.e., <2 mm) basis. All elemental analysis results reported on an oven-dry (105 °C [220 °F]) basis.

[2] USDA soil textural classification.

2.2 Proctor density measurements

Samples of different density for each soil type were prepared by placing 5 lifts (i.e., layers) of soil, approximately 900 g (1.98 lb) of material, into steel 152.4 mm (6 in.) diameter Proctor molds. For a specific test run that required a particular density, the Proctor mold was then placed into a

Durham Geo Enterprises S-335 Compactor. Each lift of soil was pneumatically hammered to the desired blow count (derived from the Proctor density curves for each soil type [Figure 5]) by using a 44.48 N (10 lb) rammer dropped from a height 457.2 mm (18 in.), producing a compactive force of 2700 kN-m/mm^3 (56,000 ft-lb/ft^3) following method ASTM D1557-12 (ASTM 2012a). Each lift was compacted with 25 blows. The total mass of soil in the Proctor mold was approximately 4500 g (9.92 lb). The weight of the mold and wet soil was determined. Soil dry-density curves were obtained for all soils by using the above method to enable selection of particular density material for use in spectrometer measurements (Figure 4).

Prior to each compaction or bulking test, the soil sample was dried overnight in an oven at a temperature of 37°C (100°F) to remove any moisture. Then, the desired amount of tap water was added to the 5000 g (11 lb) soil, mixed, and allowed to equilibrate for 24 hr in a covered plastic container to achieve the designated moisture content. A small portion of this same wet soil, approximately 150 g (0.33 lb), was weighed into a preweighed aluminum boat. This material was then placed in the oven to dry overnight. The dried soil was weighed and the weight of the aluminum boat subtracted to yield the weight of the dry soil (W_{ds}). The weight of the dry soil was subtracted from the wet soil to determine the weight of the water (W_w). The water content, w, was determined by the following equation:

$$w = [(W_w - W_{ds})/W_{ds}] \times 100 \quad (7)$$

where

w = water content,
W_w = weight of the water, and
W_{ds} = weight of the dry soil.

2.3 Gamma-ray spectrometer soil measurements

After preparation of a soil sample in the Proctor mold, the mold was placed into the center of a lead-lined enclosure (Figure 6). The gamma spectrometer was then positioned at a distance 5 cm (2 in.) above the surface of the soil and centered.

Figure 6. A Proctor mold within the lead-shield box.

Analysis consisted of using a Canberra Osprey 2x2 NaI Gamma Spectrometer (Figure 7) and Gamma Acquisition and Analysis software. The acquisition interval was 4 hr and generally followed the procedures outlined in ASTM C1402 (ASTM 2009).

Figure 7. Canberra Osprey NaI Gamma Spectrometer.

Prior to the first analysis of the day, the europium-155–sodium-22 (^{155}Eu-^{22}Na) check source was attached to the detector, and a check source analysis was performed. Following the use of the ^{155}Eu-^{22}Na check source, potassium chloride was analyzed to check the ^{40}K peak. If the ^{40}K peak is not identified correctly (i.e., only half the peak is read once collection is complete), an electrical gain shift may have occurred in the detector. A shift in gain can also be detected during the check source test; however, because

the gamma range of the electromagnetic spectrum is nonlinear, it is most important to center the ^{40}K peak compared to the ^{155}Eu and ^{22}Na peaks. This is normal over time and can be corrected by adjusting the fine gain setting on the detector (using the MCA>Adjust>Gain [radio button] in the software) and by using the check source and the potassium source to track the movement of the ^{155}Eu, ^{22}Na, and ^{40}K peaks, which should be centered at 252, 1274.5, and 1460 kilo-electron volt (keV) respectively. Figure 8 is an example of a typical spectrum for a soil sample showing a^{40}K peak at 1460 keV.

Figure 8. Example of a typical spectrum for soil showing a ^{40}K peak at 1460 keV.

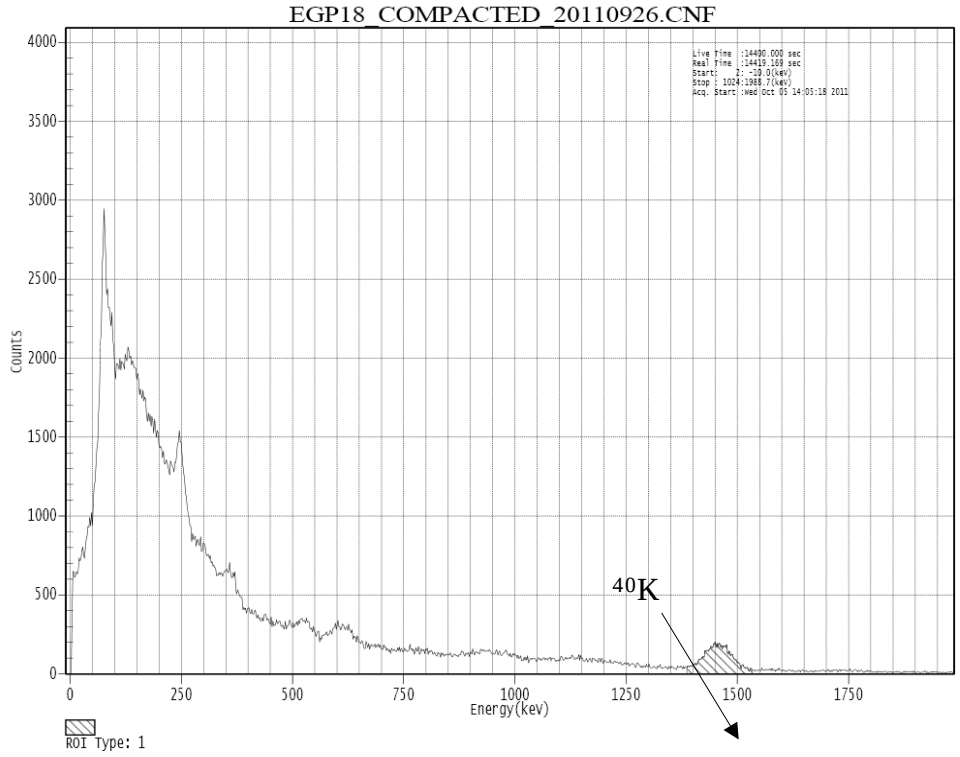

2.4 Data reduction and analysis

Raw data consisted of spectra for each soil treatment, from which intensity (detector counts) and area of the ^{40}K gamma-ray peak was extracted and 40K activity calculated using the instrument software. Soil bulk density for each treatment on an oven-dry (105°C [221°F]) basis was calculated for each treatment (i.e., spectra collection) from the volume of moist soil in the Proctor mold at a given compaction treatment and oven-dry weight of the soil (i.e., the "Calc. Dry ρ" variable in Table 2). Soil water content was also recorded for each treatment (i.e., "Actual Moist." variable in Table 2),

and changing soil water content was one of the treatment variables analyzed. A multivariate dataset consisting of 12 soil properties and three dependent variables, peak intensity, peak area, and ^{40}K activity, was statistically analyzed within the parameters of the experimental design by using JMP ver. 10 statistical software to look for significant relationships.

Table 2. Correlation matrix of gamma-ray project study data.

Correlations														
	Actual Moist.	Wet Soil Mass	Dry Soil Mass	Calc. Dry ρ	Peak Area	Contin. Counts	K-40 Activity	Sand	Silt	Clay	Fe2O3	Al203	SiO2	K
Actual Moist.	1.0000	0.3110	-0.3720	-0.1580	-0.3754	0.2173	-0.2643	-0.8055	0.6089	0.8434	0.6628	0.2752	0.3929	-0.5304
Wet Soil Mass	0.3110	1.0000	0.7661	0.4003	-0.2798	0.1893	-0.2264	-0.4735	0.4337	0.4127	0.5073	-0.2062	0.5029	-0.5451
Dry Soil Mass	-0.3720	0.7661	1.0000	0.4980	-0.0209	0.0372	-0.0437	0.0827	0.0153	-0.1721	0.0504	-0.3939	0.2269	-0.1745
Calc. Dry ρ	-0.1580	0.4003	0.4980	1.0000	-0.5075	-0.5744	-0.6463	0.0467	-0.0012	-0.0877	0.0004	-0.1101	0.0293	-0.0118
Peak Area	-0.3754	-0.2798	-0.0209	-0.5075	1.0000	0.5734	0.9506	0.4156	-0.3744	-0.3729	-0.4736	0.3426	-0.6078	0.6270
Contin. Counts	0.2173	0.1893	0.0372	-0.5744	0.5734	1.0000	0.7306	-0.3399	0.3299	0.2669	0.3019	0.2215	-0.0244	-0.0468
K-40 Activity	-0.2643	-0.2264	-0.0437	-0.6463	0.9506	0.7306	1.0000	0.2768	-0.2355	-0.2648	-0.3054	0.2189	-0.4122	0.4257
Sand	-0.8055	-0.4735	0.0827	0.0467	0.4156	-0.3399	0.2768	1.0000	-0.9072	-0.8689	-0.9319	-0.2418	-0.4066	0.5697
Silt	0.6089	0.4337	0.0153	-0.0012	-0.3744	0.3299	-0.2355	-0.9072	1.0000	0.5801	0.9777	0.0801	0.2958	-0.4324
Clay	0.8434	0.4127	-0.1721	-0.0877	-0.3729	0.2669	-0.2648	-0.8689	0.5801	1.0000	0.6575	0.3575	0.4552	-0.6084
Fe2O3	0.6628	0.5073	0.0504	0.0004	-0.4736	0.3019	-0.3054	-0.9319	0.9777	0.6575	1.0000	-0.0436	0.4866	-0.6120
Al203	0.2752	-0.2062	-0.3939	-0.1101	0.3426	0.2215	0.2189	-0.2418	0.0801	0.3575	-0.0436	1.0000	-0.6624	0.5229
SiO2	0.3929	0.5029	0.2269	0.0293	-0.6078	-0.0244	-0.4122	-0.4066	0.2958	0.4552	0.4866	-0.6624	1.0000	-0.9813
K	-0.5304	-0.5451	-0.1745	-0.0118	0.6270	-0.0468	0.4257	0.5697	-0.4324	-0.6084	-0.6120	0.5229	-0.9813	1.0000

3 Results and Discussion

3.1 Compaction state and ^{40}K gamma-ray emission from the soil surface

The primary objective of the study was to determine if there is a measurable relationship between soil ^{40}K activity (i.e., "K-40 Activity" variable in Table 2) and soil compaction state as quantified by the dry density of the soil (i.e., "Calc. Dry ρ" variable in Table 2). The ^{40}K activity of a soil is a reflection of the potassium content of the soil (Figure 9). Because most soil types contain potassium, using ^{40}K activity as a possible indicator of human–terrain interactions appears viable.

Figure 9 shows the ^{40}K activity of the four soils as a direct function of the potassium content for the soils in both a compacted and an uncompacted state. Figure 9 shows a distinct difference between the ^{40}K activity of compacted versus uncompacted soil. There were two statistically significant (α = 0.05 level) regression relationships, one for each of the respective compaction states.

$$^{40}\text{K activity} = 17695.01 + 2.60 * \text{K}, \quad R^2 = 0.77 \quad \text{compacted}$$

$$^{40}\text{K activity} = 33633.81 + 2.79 * \text{K}, \quad R^2 = 0.61 \quad \text{uncompacted}$$

The compacted soil has a significantly lower ^{40}K activity than the uncompacted soil, likely because of the limitations on recoil pathways. The compacted soil has a greater proportion of relatively high attenuating soil particles per unit cross-sectional area than does the uncompacted soil (Figure 3). Uncompacted soil, meanwhile, has a relatively open pore structure with more pore space per unit cross-sectional area than the compacted soil. This means a greater probability of low-attenuating air-filled pores being encountered by ^{40}K gamma-ray photons on their way to the soil surface in the uncompacted soil. The pore space in a compacted soil has been reduced in volume and increased in tortuosity relative to the uncompacted state, thereby reducing the ^{40}K emissions detectable at the soil surface.

Because most soil types contain potassium, using ^{40}K activity as a possible indicator of human–terrain interactions appears viable as the emission

spectra were sensitive enough across a range of soil potassium content to statistically discriminate compacted versus uncompacted soil material.

Figure 9. ^{40}K activity (pCi/g) versus potassium content (mg/kg) of compacted soil (*blue*) and uncompacted soil (*red*).

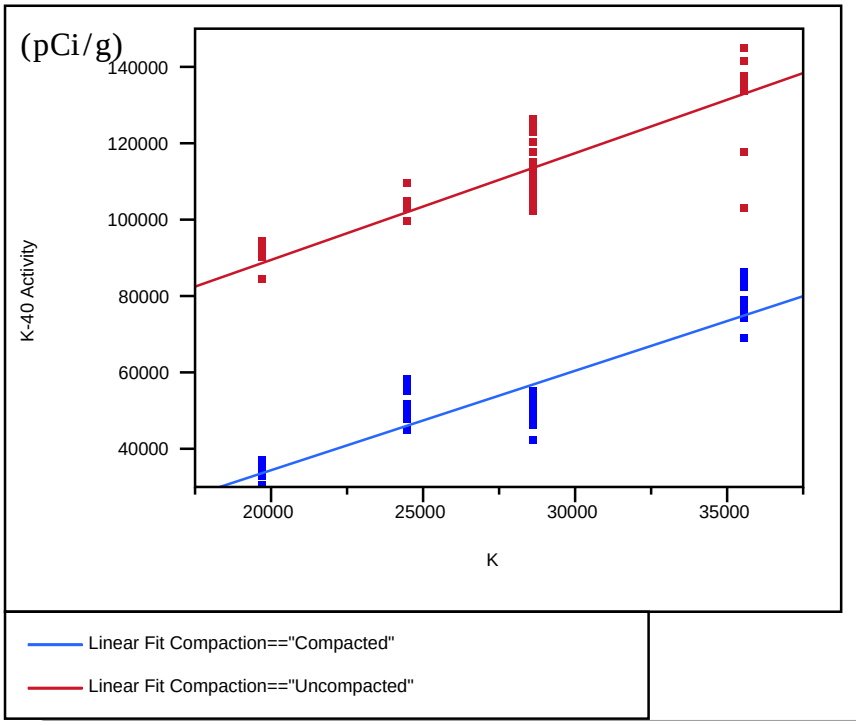

Figure 10 shows similar information, but the difference in ^{40}K activity is plotted for the compacted and uncompacted state of each soil type. The results demonstrate that for each of the four soils tested, a statistically significant difference exists between the ^{40}K activity of uncompacted versus compacted soil across the range of soil potassium contents. However, as shown by the South Bin soil, there is some overlap that might interfere with attributing ^{40}K activity to compaction state alone. This suggests that a knowledge of soil potassium content or other compositional variables may be necessary to irrefutably attribute ^{40}K activity to bulk-density differences, particularly if a time series of data is not available or fine-scale variability is inconclusive relative to the macroscale variability of the ^{40}K emissions. To investigate this possibility further, analysis of the relationship of all the variables measured to the ^{40}K activity was conducted.

Figure 10. ^{40}K (K-40) activity (pCi/g) for four soils by degree of compaction. Compacted soil is (*blue*), and uncompacted soil is (*red*).

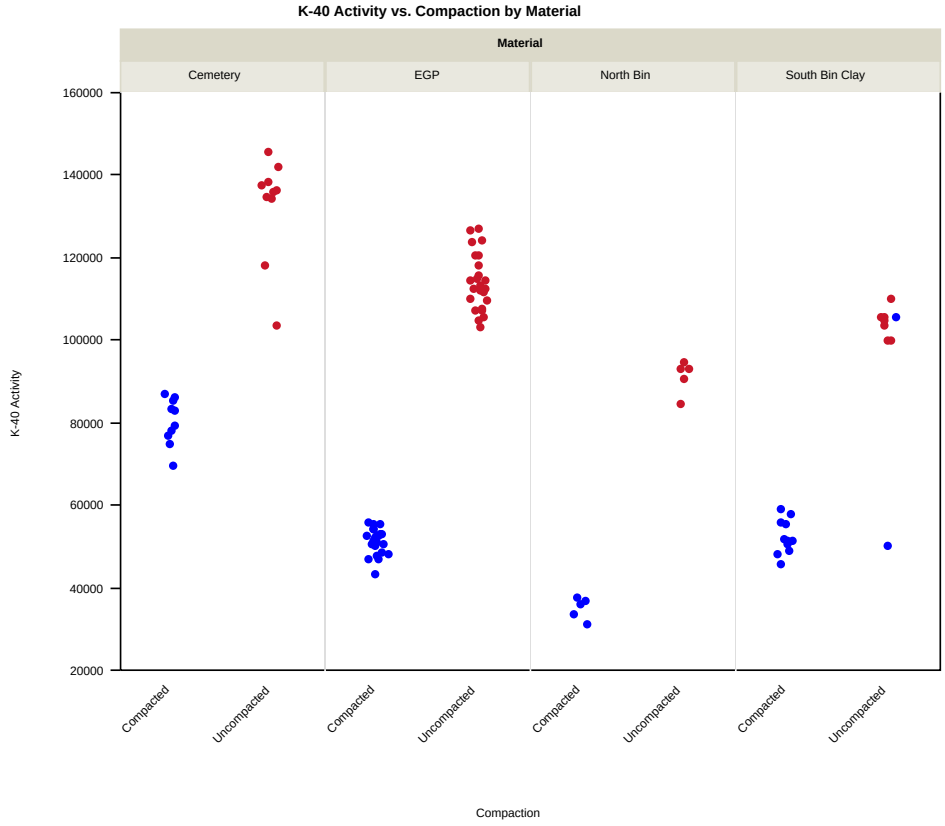

3.2 Soil composition and ^{40}K gamma-ray emissions from the soil surface

It was postulated at the start of the study that variation in soil composition, particularly in the soil potassium content, might be a significant interference confounding attribution of soil ^{40}K activity to soil compaction state alone. For example, the Cemetery soil had the highest ^{40}K activity of the four soils tested (Figure 10) but also had the highest potassium content (Table 1). Despite this fact, compaction state was still differentiable by soil ^{40}K activity for all but the North Bin soil in some cases (Figure 10). This warranted a more in-depth evaluation of the variables and their influence on the overall variance in soil ^{40}K activity and its proxies (i.e., peak area and peak counts).

For the dataset as a whole, the variable that appeared most responsible for the differences in ^{40}K gamma-ray emissions between the compacted and uncompacted soil was soil bulk density (i.e., "Calc. Dry ρ" variable in Table 2), there being a −0.6463 correlation coefficient between the calculated

dry density and ^{40}K activity (Table 2) while the correlation coefficient between ^{40}K activity and soil K content was lower, 0.4257 (Table 2). The inverse relationship between "Calc. Dry ρ" and "K-40 Activity" (Table 2) is consistent with the conceptual underpinnings (see Figure 3) and the literature indicating increased soil density blocks the path or attenuates gamma-ray release out of potassium-bearing minerals and into the surrounding soil matrix and ultimately into the air above the soil surface. Again, the strength of this relationship was somewhat surprising and suggests that interaction among the entire suite of variables may be more complex than originally surmised.

3.2.1 Principle components analysis

Because many of the variables (Table 2) were correlated, a principle components analysis was performed to see if the variables grouped into distinct components that differed significantly in explaining the overall variance of the dataset. The results are presented in the form of a loading plot (Figure 11).

Figure 11. Loading plot of principal component results.

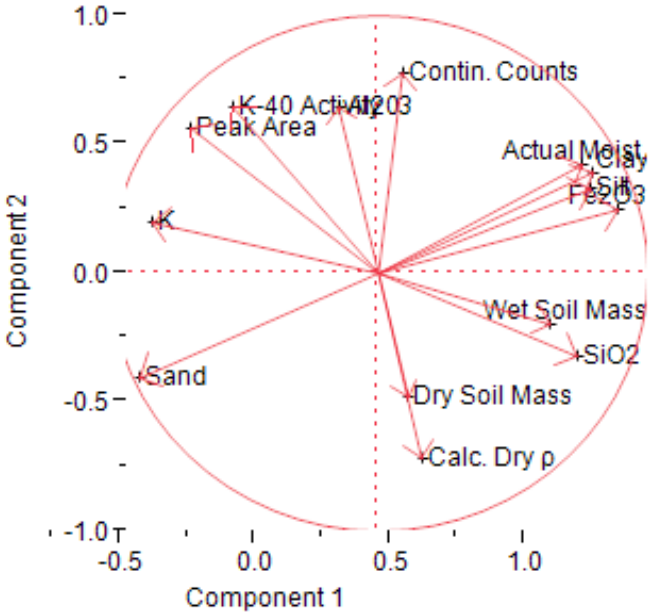

The circle represents a unit circle (i.e., radius 1) and is the square of the normalized variance. Vectors (i.e., variables) more closely aligned with a particular component axis are loaded more heavily by that principle component while the length of the respective vector is proportional (i.e., the squared length of the vector) to the variance contributed by that variable

(again, normalized to 1.0). Vectors that plot in opposite quadrants are inversely related.

The separate soil particle size fractions are heavily loaded by Principal Component 1 (i.e., the variance in these variables explains a significant portion of the overall variance in the dataset). As would be expected, there is an inverse relationship between the fines (silt and clay fractions) and the sand fraction (Figure 11). It is also interesting to note of the elemental composition variables, the Fe_2O_3 is highly correlated with the silt and clay particle size fractions and highly negatively correlated with the sand fraction (Table 2 and Figure 11). This is consistent with the iron likely being bound up in secondary iron oxides that are a product of weathering and exist as discrete fine particles or as coatings on finer particles rather than being a constituent of any primary or secondary iron-bearing minerals inherited from the soil parent material.

Of the other elemental composition variables, the potassium content is also heavily loaded by Principal Component 1, as is the SiO_2 content, and is inversely related to the SiO_2 content with a very highly negative −0.9813 correlation coefficient (Table 2). Potassium, however, does covary to some extent with the Al_2O_3 content (Table 2). This might be explained if much of the SiO_2 is tied up in quartz in the coarser fractions while much of the potassium in the soils is probably tied up in potassium-bearing aluminosilicate mineral phases, likely also in the coarser fractions judging by the +0.5697 correlation coefficient with the sand fraction and the negative correlations with silt and clay fractions (see Table 2).

The soil compositional variables, loaded heavily by Principal Component 1, explain a significant portion of the overall dataset variability as seen by the lengths of their variance vectors (Figure 11). Also, Principal Component 1 loads most heavily on soil moisture while Principal Component 2 loads most heavily on ^{40}K activity. This suggests that interferences from soil water content in attribution of ^{40}K activity to bulk density may not be as significant as once thought and does not obscure relationships between soil density and ^{40}K activity.

The variables being loaded by Principal Component 2 explain the portion of the overall dataset variability over and above what the compositional variables explain. Principal Component 2 loads most heavily with the ^{40}K activity and associated variables (e.g., peak area and continuous counts)

and in particular the soil bulk density (i.e., Calc. Dry ρ). This separation of loading with soil potassium content being loaded by Principal Component 1 while soil bulk density and ^{40}K activity and related measures are loaded by Principal Component 2 suggests that the soil potassium activity is more related to soil density or compaction state than to soil potassium content. The inverse relationship between measures of ^{40}K activity and soil bulk density (Figure 11) is clearly evident, which is consistent with the conceptual model (see Figure 3) and the literature. Soil potassium content is not very strongly correlated with ^{40}K activity (correlation coefficient of about +0.4257 in Table 2) and therefore does not appear to present a significant interference in attributing changes in soil ^{40}K activity to changes in soil bulk density, at least for the soil materials studied.

Figure 12 is a scatter plot of the entire dataset. There is no significant linear relationship between ^{40}K activity and soil bulk density (i.e., Calc. Dry ρ) across the dataset as a whole. A regression line fit to the data had a very low R^2 value of 0.28 and suggests that density has no predictive or explanatory value (Figure 12). However, a correlation analysis supports that an inverse relationship is apparent between ^{40}K activity and the dry density of the soil (i.e., as the soil density increases, the ^{40}K activity decreases [negative correlation of −0.65]) (Table 2). This finding is consistent with literature indicating that increased soil density blocks the path or attenuates gamma-ray release out of potassium-bearing mineral and into the surrounding soil matrix or air above the soil. The results also indicate that the potassium content of the soil is related to the amount of sand (positive correlation of 0.57) and negatively correlated with clay (−0.61) (Table 2). Further, the sand consists of Al_2O_3 minerals that contain potassium (correlation of 0.53) and are not associated with Fe_2O_3 or SiO_2 (clay) mineral assemblages (negative correlations of −0.61 and −0.98, respectively). This finding is a bit surprising as the expectation was that a positive relationship exists between the clay content of the soil and the ^{40}K activity. The basis for this expectation was that many clay soils contain high-potassium-content minerals.

The Figure 12 scatter plot does show, however, the range of Calc. Dry ρ (in kg/m^3) and the corresponding range of ^{40}K activity counts measured in the testing. The density spanned a wide range of values, from almost the maximum dry density of some of the soils (Table 2) to around 1 kg/m^3, which exceeds the range of bulk density typically encountered in many field soils.

Figure 12. ^{40}K activity (pCi/g) versus the calculated dry density (g/cm^3) of soil.

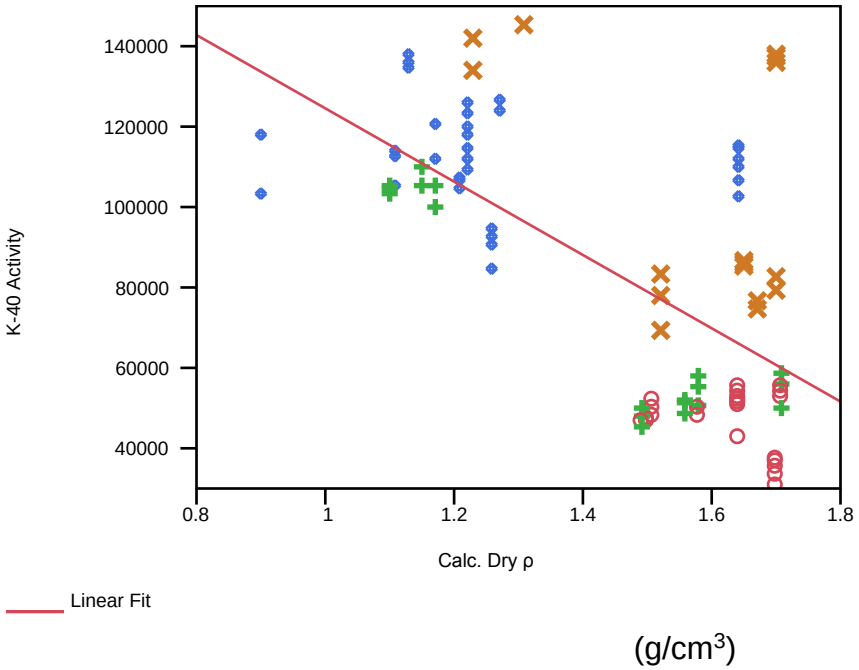

Figure 12 indicates that attempting to generalize across a range of soil types a single continuous relationship between ^{40}K activity and soil bulk density is not possible. However, it is still clear that soil ^{40}K activity does discriminate compacted versus uncompacted state for a given soil (see Figures 9 and 10). This suggests that at macroscales (i.e., over large areas of terrain) with a variety of soil types, one cannot a priori attribute a particular soil ^{40}K activity to a particular soil bulk-density state that indicates a disturbance. However, at what Christakos (1992) refers to as microscales (i.e., small areas of terrain) variance of soil ^{40}K activity is probably a good indicator of soil compaction state as indicated by bulk density and thus may be a useful soil-disturbance metric. Differences in the variance structure of a random field of soil ^{40}K activity going from the macro- to the microscales may essentially control for the variables that are loaded heavily by Principal Component 1, such as potassium content, soil particle size distribution, and soil moisture content (Figure 11). This allows the variance of those variables loaded more heavily by Principal Component 2, potassium activity and soil density, to be more sensitive to soil-disturbance impacts.

3.2.2 Cluster analysis

A hierarchical cluster analysis was performed (Figure 13) to see if it was possible to further sort out the interaction and relationships of the different variables. A cluster analysis essentially groups samples that are near each other in the sample space in terms of the variables analyzed, resulting

in a smaller number of groups of samples that, hopefully, differ significantly from one another (Figure 13).

Figure 13. Hierarchical clustering analysis for the study data.

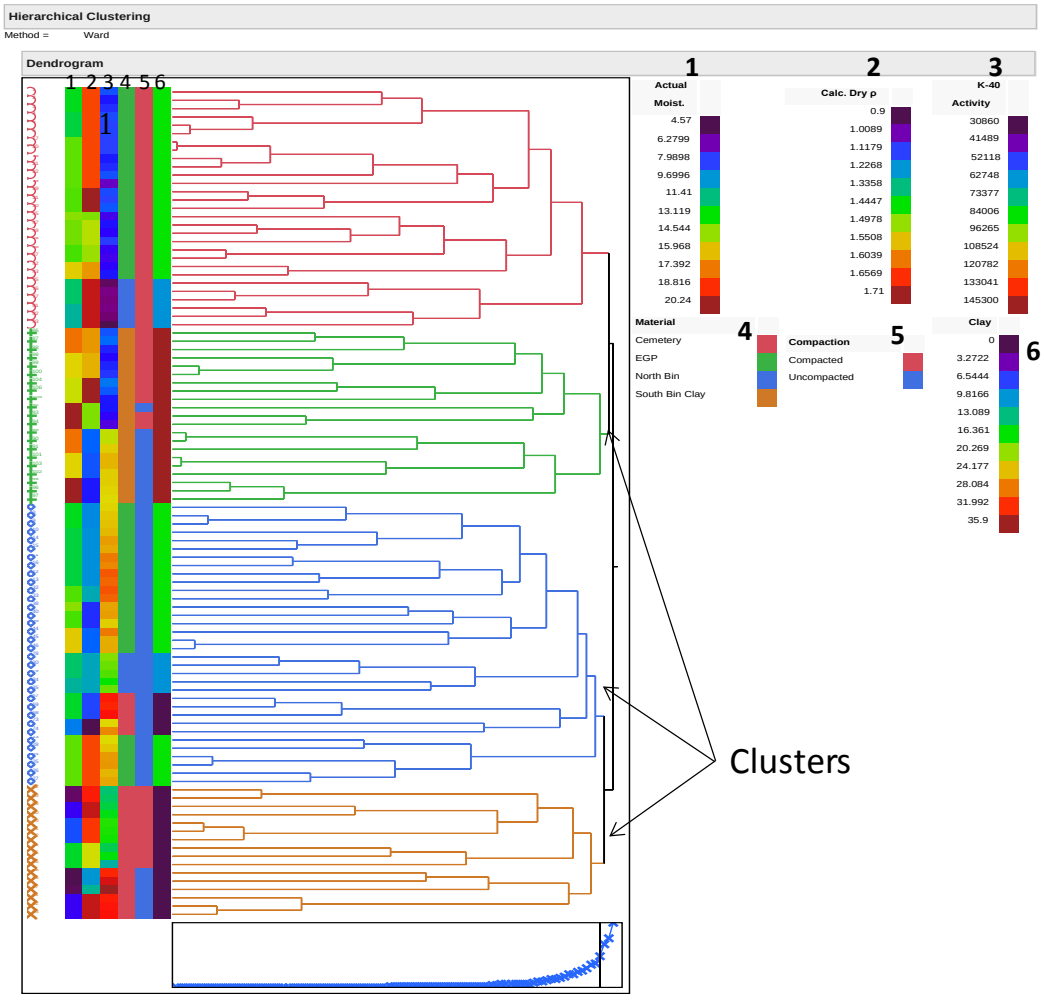

Variables considered were (1) Actual Moist. (i.e., soil moisture content), (2) Calc. Dry ρ, (3) K-40 Activity, (4) Material (i.e., soil type), (5) compaction (i.e., compacted or uncompacted), and (6) clay (clay fraction). Soil potassium content was specifically excluded from this analysis to better observe the interaction of these other variables. It seems clear that the clay content, column 6 in Figure 13, as measured by the clay fraction (Table 1), explains the green and brown sample clusters and agrees with column 4, soil type, the green cluster being the treatments (samples) with the South Bin silty clay loam soil and the brown cluster being the treatments with the Cemetery sand (Table 1).

The red and blue clusters appear to be differentiated by their Calculated Dry Density, column 2, with the red cluster having higher densities than the blue cluster. Soil compaction state also differentiates these clusters (column 5), red being compacted and blue being uncompacted. Actual Moist. (i.e., soil moisture content), column 1, also appears to be a significant differentiating variable in the clustering with the brown cluster having a lower moisture content than the blue and red clusters, which have moderate moisture levels, and the green cluster, which has the highest moisture content. Table 3 somewhat subjectively summarizes the groups.

Table 3. Differentiating variables of the cluster analysis groups.

Cluster Color	Actual Moist.	Calc. Dry ρ	^{40}K Activity	Material	Compaction	Clay
Red	Int. moist.	High ρ	low		compacted	
Green	High moist.	Low intermediate	Low intermediate	South Bin Clay (silica texture)		high
Blue	Int. moist.	Low ρ	intermediate		uncompacted	
Brown	Low moist.	High ρ	high	Cemetery (sand texture)		low

The green and brown groups are clustered around stable soil properties; and the two groups are differentiated by those properties, such as the green clusters have a high clay content, fine texture, and high moisture content. The brown cluster of data consists of soils with low clay content, coarse texture, and low moisture content. The red and green groups are clustered around use-dependent temporal properties that were treatment variables or functions thereof. The red group has a high density, low ^{40}K activity, and is compacted, while the blue group has a low density, intermediate ^{40}K activity, and is uncompacted.

This suggests that soils with coarse textures, such as sandy soils, or finer textures, such as clayey soils (i.e., the green and brown group clusters), may have inherent physical properties that can control or limit compaction state and associated ^{40}K activity to a significant extent. Conversely, the red and blue clusters represent soils with fewer constraints and may be more responsive to soil density changes and subsequent ^{40}K activity variation as a result of disturbance. Again, this suggests that variation of ^{40}K activity on the macroscale may be influenced by stable static soil properties in addition to disturbance, while narrowing observations to a smaller area and focusing on the microscale might help control such extraneous sources of

variation and allow greater attribution of ^{40}K activity to soil density or compaction state alone.

3.2.3 Correlation analysis

Finally, a weak positive correlation (0.43) is evident between the potassium content of the soil and the ^{40}K activity (Table 2). Again, this is a surprise because the expectation was for a strong relationship between the potassium content of the soil and the ^{40}K activity. The weaker correlation suggests other variables may be responsible for attenuating the potassium content linkage to ^{40}K activity.

These same correlation relationships are evident when performing a principal component analysis of the data and presenting the results in a loading plot. The results show that Principal Component 1 is a function of a positive relationship between ^{40}K activity, potassium soil content, Al_2O_3, sand, and peak area. Peak area is a redundant measurement similar to ^{40}K activity. Sand has a significant Al_2O_3 content, so a positive relationship between the two is not surprising. The ^{40}K activity is also inversely related to dry-soil density, SiO_2, soil moisture, Fe_2O_3, silt, and clay.

Both increased soil moisture and dry soil density have the potential to attenuate the ^{40}K activity. The inverse relationship with clay and silt suggests that sandy soils have a greater ^{40}K activity. However, the finding is contrary to our expectation where clays are known to have a high potassium content and presumably ^{40}K activity. It is possible that other variables, possibly soil density or soil moisture, are confounding this relationship. Clay or silty soils are more easily compacted (higher soil density) and can hold a greater degree of soil moisture, which would have a tendency to attenuate a ^{40}K signature.

Principal Component 2 indicates that ^{40}K activity, potassium content, Al_2O_3, moisture, silt and clay, and Fe_2O_3 are similarly related and inversely related to sand, density, and SiO_2. In addition to dry soil density, the results indicate other variables are potentially influencing the measured ^{40}K activity of the soil.

4 Conclusions

This study established at lab scale the phenomenology of in situ gamma-ray emissions from the soil surface to detect differences in soil compaction state. Standoff measures of ^{40}K activity decrease with an increase in soil bulk density or between an uncompacted and compacted soil state. In addition, standoff passive soil ^{40}K gamma emissions are a repeatable, sensitive indicator of soil fabric disturbance that results in changes in soil bulk density when soil materials are of similar composition. Soil compositional variables do impact the nature of the ^{40}K activity versus bulk-density relationship. Changes in bulk density contribute enough variance in the overall data that there is not one simple linear relationship between soil bulk density and ^{40}K activity that characterizes all soils. Neither soil potassium content nor soil moisture content, however, were significant enough interferences to overwhelm the soil ^{40}K activity and to prevent its use as a metric of soil compaction state

Relationships observed between soil potassium content, ^{40}K activity, soil bulk density, and soil moisture content suggest that it may be possible to correct for potential interferences from soil potassium content and soil moisture content if needed by adjusting the spatial scale of measurements (focusing on microscale variability rather than macroscale) or by using time series of measurements to account for effects from very temporally variable parameters such as soil water content.

The phenomenology of the use of in situ soil ^{40}K activity to infer soil compaction state is significant enough to explore increasing instrumentation sensitivity (e.g., HPGe based detector) or other methodological enhancements (e.g., spatiotemporal sequenced measurements over short distances) that would increase standoff distance, shorten spectra collection times, and enhance detection of microscale patterns. This would increase the utility of this method for field application in real time.

References

ASTM. 2012a. *Standard Test Methods for Laboratory Compaction Characteristics of Soil Using Modified Effort*. ASTM D1557-12. West Conshohocken, PA: ASTM International.

———. 2012b. *Standard Test Methods for Laboratory Compaction Characteristics of Soil Using Standard Effort*. ASTM D698-12. West Conshohocken, PA: ASTM International.

———. 2009. *Standard Guide for High-Resolution Gamma-Ray Spectrometry of Soil Samples*. ASTM C1402-04. West Conshohocken, PA: ASTM International.

———. 2007. *Standard Test Method for Particle-Size Analysis of Soils*. ASTM D422-63. West Conshohocken, PA: ASTM International.

Blum, P. 1997. *Physical Properties Handbook: A Guide to the Shipboard Measurement of Physical Properties of Deep-Sea Cores*. Ocean Drilling Project Tech. Note 26. http://www-odp.tamu.edu/publications/tnotes/tn26/TOC.HTM.

Brewer, R. 1976. *Fabric and Mineral Analysis of Soils*. Huntington, NY: R. E. Krieger Publishing Company.

Christakos, G. 1992. *Random Field Models in Earth Sciences*. New York, NY: Academic Press, Inc.

Diaz-Zorita, M., J. H. Grove, and E. Perfect. 2001. Laboratory Compaction of Soils Using a Small Mold Procedure. *Soil Science Society of America Journal* 65:1593–1598.

Dickson, B. L., and K. M. Scott. 1997. Interpretation of Aerial Gamma-Ray Surveys—Adding the Geochemical Factors. *Journal of Australian Geology and Geophysics* 17 (2): 187–200.

Feng, T. C., J. Y. Jia, B. Lopng, C. Y. Su, R. Wu, and J. P. Cheng. 2008. Delaminated Method to Determine the Depth Distribution of ^{152}Eu in Soil by In-Situ HPGe γ Spectrometry. *Nuclear Instruments and Methods in Physics Research Section A* 597:192–197.

Food and Agriculture Organization (FAO). 1998. *Watershed Management Field Manual: Road Design and Construction in Sensitive Watersheds*. FAO Conservation Guide 13/5. Rome, Italy: Food and Agriculture Organization of the United Nations.

Hendriks, P. H. G. M., J. Limburg, and R. J. de Meijer. 2001. Full-Spectrum Analysis of Natural γ-Ray Spectra. *Journal of Environmental Radioactivity* 53:365–380.

Hopkins, R. C. 1996. *An Aerial Radiological Survey of Frenchman Flat at the Nevada Test Site*. DOE/NV/11718-012. Bechtel, Nevada: U.S. Department of Energy Remote Sensing Laboratory.

Jones, W. K., and Z. T. R. Carroll. 1983. Error Analysis of Airborne Gamma Radiation Soil Moisture Measurements. *Agricultural Meteorology* 28:19–30.

Kinno, M., K. Kimura, T. Ishikawa, T. Miura, S. Ishihama, N. Hayasaka, and T. Nakamura. 2002. Correlation Between Tritium and ^{152}Eu Induced in Various Types of Concrete by Thermal Neutron Irradiation. Journal of Nuclear Science Technology 39:215–225.

Kouzes, R. T., E. R. Siciliano, J. H. Ely, P. E. Keller, and R. J. McConn. 2007. Passive Neutron Detection at Borders. In *IEEE Nuclear Science Symposium Conference Record, 27 October–3 November, Honolulu, Hawaii*, 1: 1115–1119.

Lyons, C., and T. Hendricks. 2006. *An Aerial Radiological Survey of the Yucca Mountain Project Proposed Land Withdrawal and Adjacent Areas.* DOE/NV/11718-1258. Las Vegas, NV: U.S. Department of Energy.

Minty, B. R. S. 1997. Fundamentals of Airborne Gamma-Ray Spectrometry. *Journal of Australian Geology and Geophysics* 17 (2): 39–50.

Paine, J. G., and B. R. S. Minty. 2005. Airborne Hydrogeophysics. In *Hydrogeophysics*, ed. Y. Rubin and S. S. Hubbard, 33–357. The Netherlands: Springer, Water Science and Technology Library.

Phogat, V. K., L. A. G. Aylmore, and R. D. Schuller. 1991. Simultaneous Measurement of the Spatial Distribution of Soil Water Content and Bulk Density. *Soil Science Society American Journal* 55:908–915.

Rossel, R. A. V., H. J. Taylor, and A. B. McBratney. 2007. Multivariate Calibration of Hyperspectral γ–Ray Energy Spectra for Proximal Soil Sensing. *European Journal of Soil Science* 58:343–353.

Santo Júnior, J. A. D., J. J. R. F. Cardoso, C. M. da Silva, S. V. Silveira, and R. dos Santos Amaral. 2005. Analysis of the ^{40}K Levels in Soil Using Gamma Spectrometry. *Brazilian Archives of Biology and Technology* 48:221–228. doi:10.1590/S1516-89132005000700033.

Soil Survey Staff. 1951. *Soil Survey Manual*. U. S. Department of Agricultural Handbook No. 18. Washington, DC: U.S. Department of Agriculture.

USEPA (U.S. Environmental Protection Agency). 2016. Chapter 3: Inorganic Analytes. In *Test Methods for Evaluating Solid Waste*. SW-846. https://www.epa.gov/hw-sw846/chapter-three-sw-846-compendium-inorganic-analytes (accessed January 2016).

Vanmarcke, E. 1983. *Random Fields: Analysis and Synthesis*. Cambridge, MA: MIT Press.

Vo, D. T., and P. A. Russo. 2002. *Comparisons of Portable Digital Spectrometer Systems*. LA-13895-MS. Los Alamos, NM: Los Alamos National Laboratory.

Wilford, J. R., P. N. Bierwirth, and M. A. Craig. 1997. Application of Airborne Gamma-Ray Spectrometry in Soil/Regolith Mapping and Applied Geomorphology. *Journal of Australian Geology of Geophysics* 17 (2): 201–216.

Appendix A: Additional Chemistry Data

Table A-1. Elementa results (mg/kg) for the four test soils.

Sample Name	As	Ba	Ca	Cr	Co	Cu	Mg	Mn	Ni	P	K	Na	Tl	Ti	V	Zn
Cemetery	105	1197	12519	271	12481	<50	2221	274	<50	378	35500	31988	125	1626	59	64
EGP	138	773	53875	140	12481	75	20331	878	51	1145	28563	26213	338	4262	110	213
South Bin	129	522	14969	155	12813	<50	12963	898	64	747	24456	25981	326	4409	115	174
North Bin	124	414	23725	251	12606	55	12656	881	65	691	19625	28494	311	4104	124	178

Table data is in units of ug/kg.

As = arsenic Ba = barium Ca = calcium Cr = chromium Co = cobalt Cu = copper

Mg = magnesium Mn = manganese Ni = nickel P = phosphorus K = potassium Na = sodium

Tl = thallium Ti= titanium V = vanadium Zn = zinc

REPORT DOCUMENTATION PAGE

Form Approved
OMB No. 0704-0188

1. REPORT DATE *(DD-MM-YYYY)*	**2. REPORT TYPE**	**3. DATES COVERED** *(From - To)*
August 2016	Technical Report/Final	

4. TITLE AND SUBTITLE

Passive Gamma-Ray Emission for Soil-Disturbance Detection

5a. CONTRACT NUMBER

5b. GRANT NUMBER

5c. PROGRAM ELEMENT NUMBER

6. AUTHOR(S)

Jay L. Clausen, Terrance Sobecki, Alexis L. Coplin, Terry D. Melendy, and Troy Arnold

5d. PROJECT NUMBER
PE0602784 Project 855

5e. TASK NUMBER

5f. WORK UNIT NUMBER

7. PERFORMING ORGANIZATION NAME(S) AND ADDRESS(ES)

U.S. Army Engineer Research and Development Center (ERDC)
Cold Regions Research and Engineering Laboratory (CRREL)
72 Lyme Road
Hanover, NH 03755-1290

8. PERFORMING ORGANIZATION REPORT NUMBER

ERDC/CRREL TR-16-10

9. SPONSORING / MONITORING AGENCY NAME(S) AND ADDRESS(ES)

Headquarters, U.S. Army Corps of Engineers
Washington, DC 20314-1000

10. SPONSOR/MONITOR'S ACRONYM(S)

11. SPONSOR/MONITOR'S REPORT NUMBER(S)

12. DISTRIBUTION / AVAILABILITY STATEMENT

Approved for public release; distribution is unlimited.

13. SUPPLEMENTARY NOTES

14. ABSTRACT

Human–terrain interactions, such as trafficking and excavation, cause changes to soil bulk density and porosity via compaction or mechanical bulking. The degree of compaction, as measured by bulk density, is a physical indicator of changing patterns of human–terrain interaction. Because soil radionuclide activity is a function of the mass content of the radionuclide and the volume of soil, the spectral signature of the naturally occurring soil radioisotope Potassium-40 (^{40}K) should be sensitive to changes in the soil bulk density and reflect the soil's disturbance history. If natural variations from geology and soil texture are systematic and predictable, one could map spatiotemporal bulk-density changes relative to some standard state as a metric of terrain disturbance. However, the natural variation in soil ^{40}K content is unknown and may confound density determinations via radionuclide activity measurements.

This study used a handheld sodium iodide gamma-ray detector to collect in situ gamma-ray spectra of four soils as a function of their potassium content, bulk density, texture, and water content. A statistically significant difference between the ^{40}K activity of uncompacted and compacted soil suggests that in situ ^{40}K gamma-ray emissions from soils are a sensor modality useful for soil-disturbance detection.

15. SUBJECT TERMS

Gamma ray detectors, Gamma ray spectrometry, Gamma rays--Measurement, Radioactive substances in soils, Soil compaction, Soils--Density--Measurement, Soils--Electric properties, Soils--Environmental aspects, Soils--Testing

16. SECURITY CLASSIFICATION OF:			**17. LIMITATION OF ABSTRACT**	**18. NUMBER OF PAGES**	**19a. NAME OF RESPONSIBLE PERSON**
a. REPORT	**b. ABSTRACT**	**c. THIS PAGE**			**19b. TELEPHONE NUMBER** *(include area code)*
Unclassified	Unclassified	Unclassified	SAR	51	